Curie temperature of the two-band double-exchange model for manganites

Vasil Michev and Naoum Karchev*
Department of Physics, University of Sofia, 1164 Sofia, Bulgaria
(Received 26 July 2007; revised manuscript received 21 September 2007; published 6 November 2007)

We consider the two-band double-exchange model and calculate the critical temperature in the ferromagnetic regime (Curie temperature). The localized spins are represented in terms of the Schwinger bosons, and two spin-singlet Fermion operators are introduced. In terms of the new Fermi fields the on-site Hund's interactions are in a diagonal form and one accounts for them exactly. Integrating out the spin-singlet fermions we derive an effective Heisenberg-type model for a vector which describes the local orientations of the total magnetization. The transversal fluctuations of the vector are the true magnons in the theory, which is the base for Curie temperature calculation. The critical temperature is calculated employing the Schwinger-bosons mean-field theory. While approximate, this technique of calculation captures the essentials of the magnon fluctuations in the theory, and for two-dimensional systems one obtains zero Curie temperature, in accordance with the Mermin-Wagner theorem.

DOI: 10.1103/PhysRevB.76.174412 PACS number(s): 75.47.Lx, 71.27.+a, 75.30.Ds, 75.50.Cc

I. INTRODUCTION

Manganites are prominent representatives of strongly correlated systems, where the effect of correlations among electrons plays a crucial role. The growing interest in manganites is mainly due to observation of resistivity changes by many orders of magnitude upon the application of small magnetic fields, an effect that is called colossal magnetoresistance.

The attempts to properly describe the physics of these materials by means of simple perturbative methods typically fail.[1] One has to develop a technique of calculation which capture's the essential features of the compounds. The double exchange model is a widely used model for manganites.[1–3] In isolation, the ions of Mn have an active $3d$ shell with five degenerate levels. The degeneracy is presented due to rotational invariance within angular momentum $l=2$ subspace. The crystal environment results in a particular splitting of the five d orbitals (crystal field spliting) into two groups: the e_g and t_{2g} states. The electrons from the e_g sector, which form a doublet, are removed upon hole doping. The t_{2g} electrons, which form a triplet, are not affected by doping, and their population remains constant. The Hund rule enforces alignment of the three t_{2g} spins into a $S=3/2$ state. Then, the t_{2g} sector can be replaced by a localized spin at each manganese ion, reducing the complexity of the original five orbital model. The only important interaction between the two sectors is the Hund coupling between localized t_{2g} spins and mobile e_g electrons. A strong impact on the physics of manganites has the static Jahn-Teller distortion which leads to a splitting of the degenerate e_g levels.

The double exchange model has a rich phase diagram, exhibiting a variety of phases, with unusual ordering in the ground states. The procedures followed to obtain the phase diagram in one band model are different: numerical studies,[4,5] dynamical mean-field theory (DMFT),[6] and analytical calculations,[7,8] but four phases have been systematically observed: (i) antiferromagnetism (AF) at a density of mobile electrons $n=1$, (ii) ferromagnetism (FM) at intermediate electronic densities, (iii) phase separation (PS) between FM and AF phases, and (iv) spin incommensurable (IC) phase at large enough Hund coupling. The competition between spin spiral incommensurate order or phase separation and canted ferromagnetism is also a topic of intensive study.[7–9] The phase diagram becomes more rich if the orbital degeneracy is accounted for.[10,11]

The double exchange model is also used to calculate the critical temperature in the ferromagnetic regime of manganites. Predictions about Curie temperature in the one-band double-exchange model are made using the Monte Carlo (MC) technique,[4] high-temperature series expansion,[12] dynamical mean-field theory,[13] and a standard mean-field approach.[14] The most striking feature of the critical temperature as a function of fermion density is the symmetry with respect to $n=0.5$. The Curie temperature is maximized at that point, and the maximal value is different within different approaches.

Very recently the critical temperature was calculated using a two-band model taking account of the Jahn-Teller effect.[15,16] Again the characteristic feature of the temperature curves as a function of charge carrier density is the symmetry with the respect to $n=1$. The new assertion is that the Curie temperature increases with increasing interband hopping.[15]

It is impossible to require the theoretically calculated Curie temperature to be in accordance with experimental results. The models are idealized and they do not consider many important effects: phonon modes, several types of disorder, Coulomb interaction, etc. Because of that it is important to formulate theoretical criteria for the adequacy of the method of calculation. In our opinion the calculations should be in accordance with the Mermin-Wagner theorem.[17] It claims that in two dimensions there is no spontaneous magnetization at nonzero temperature. Hence, the critical temperature should be equal to zero. It is well known that Monte Carlo method of calculation does not satisfy this criteria, and a "weak z-coupling" three-dimensional (3D) system is used to mimic a 2D layer.[1] It is difficult within dynamical mean-field theory to make a difference between two- and three-dimensional systems. DMFT is a good approximation when the dimensionality goes to infinity. This made the analytical methods important even for the assessment of the numerical results.

The paper is organized as follows. In Sec. II, starting from two-band double-exchange model, we derive an effective Heisenberg-like model in terms of the vector describing the local orientations of the total magnetization. The transversal fluctuations of the vector are the true magnons in the theory. This is a base for Curie temperature calculation. Section III is devoted to phase diagrams of the model in space of Hund's constant and charge carrier density. We calculate the spin-stiffness constant as a function of density which is an important step towards understanding the Curie temperature behavior as a function of charge carrier density. The results for the Curie temperature are reported in Sec. IV. A summary in Sec. V concludes the paper. Spin-stiffness constant calculations are presented in the Appendix.

II. EFFECTIVE MODEL

We consider a two-band double-exchange model, with the Hamiltonian

$$H = -\sum_{ll'\langle ij\rangle\sigma} (t_{ll'} c^+_{il'\sigma} c_{jl\sigma} + \text{H.c.}) - 2\sum_{il} J_l \vec{S}_i \cdot \vec{s}_{il} - \mu \sum_{il} c^+_{il\sigma} c_{il\sigma}, \tag{2.1}$$

where l,l' are band indexes, i,j are site labels, σ are the spin indices, $c^+_{il\sigma}$ and $c_{il\sigma}$ are creation and destruction operators for mobile electrons, and μ is the chemical potential. s_{il} is the spin of the conduction electrons and $\mathbf{S}_i$ is the spin of the localized electrons. The sums are over all sites of a three-dimensional cubic lattice and $\langle i,j\rangle$ denotes the sum over the nearest neighbors. We denote $t_{11} \equiv t_1$, $t_{22} \equiv t_2$, and $t_{12} \equiv t_{21} \equiv t'$.

In terms of Schwinger-bosons $(\varphi_{i\sigma}, \varphi^\dagger_{i\sigma})$ the core spin operators have the following representation:

$$\vec{S}_i = \frac{1}{2} \varphi^+_{i\sigma} \vec{t}_{\sigma\sigma'} \varphi_{i\sigma'}, \quad \varphi^+_{i\sigma}\varphi_{i\sigma} = 2s \tag{2.2}$$

with the Pauli matrices (τ^x, τ^y, τ^z).

The partition function can be written as a path integral over the complex functions of the Matsubara time $\varphi_{i\sigma}(\tau)$ $[\varphi^+_{i\sigma}(\tau)]$ and Grassmann functions $c_{il\sigma}(\tau)$ $[c^+_{il\sigma}(\tau)]$:

$$\mathcal{Z}(\beta) = \int \prod_{i\sigma\tau} \frac{d\varphi^+_{i\sigma}(\tau) d\varphi_{i\sigma}(\tau)}{2\pi\imath} \prod_{il\sigma\tau} dc^+_{il\sigma}(\tau) dc_{il\sigma}(\tau) e^{-S} \tag{2.3}$$

with an action given by the expression

$$S = \int_0^\beta d\tau \Bigg\{ \sum_i [\varphi^+_{i\sigma}(\tau)\dot{\varphi}_{i\sigma}(\tau) + c^+_{il\sigma}(\tau)\dot{c}_{il\sigma}(\tau)] + h(\varphi^+, \varphi, c^+, c) \Bigg\}, \tag{2.4}$$

where β is the inverse temperature and the Hamiltonian is obtained from Eqs. (2.1) and (2.2) replacing the operators with the functions.

We introduce spin-singlet Fermi fields

$$\Psi^A_{il}(\tau) = \frac{1}{\sqrt{2s}} \varphi^+_{i\sigma}(\tau) c_{il\sigma}(\tau), \tag{2.5}$$

$$\Psi^B_{il}(\tau) = \frac{1}{\sqrt{2s}} [\varphi_{i1}(\tau) c_{il2}(\tau) - \varphi_{i2}(\tau) c_{il1}(\tau)] \tag{2.6}$$

which are U(1) gauge variant with charge −1 and 1, respectively,

$$\Psi'^A_{jl}(\tau) = e^{-i\alpha_j(\tau)} \Psi^A_{jl}(\tau), \quad \Psi'^B_{jl}(\tau) = e^{i\alpha_j(\tau)} \Psi^B_{jl}(\tau). \tag{2.7}$$

The equations (2.5) and (2.6) can be regarded as a SU(2) transformation

$$\Psi_{il\sigma} = g^+_{i\sigma\sigma'} c_{il\sigma'} \Rightarrow g^+_i = \frac{1}{\sqrt{2s}} \begin{pmatrix} \varphi^+_{i1} & \varphi^+_{i2} \\ -\varphi_{i2} & \varphi_{i1} \end{pmatrix} \tag{2.8}$$

with $\Psi^A_{il} = \Psi_{il1}$ and $\Psi^B_{il} = \Psi_{il2}$.

In terms of the new Fermi fields, electron creation and destruction operators have the form

$$c_{il1} = \frac{1}{\sqrt{2s}} (\varphi_{i1} \Psi^A_{il} - \varphi^+_{i2} \Psi^B_{il}),$$

$$c_{il2} = \frac{1}{\sqrt{2s}} (\varphi_{i2} \Psi^A_{il} + \varphi^+_{i1} \Psi^B_{il}),$$

$$c^+_{il1} = \frac{1}{\sqrt{2s}} (\varphi^+_{i1} \Psi^{+A}_{il} - \varphi_{i2} \Psi^{+B}_{il}),$$

$$c^+_{il2} = \frac{1}{\sqrt{2s}} (\varphi^+_{i2} \Psi^{+A}_{il} + \varphi_{i1} \Psi^{+B}_{il}) \tag{2.9}$$

and the spin of the conduction electrons $\mathbf{s}_{il}$ is

$$s^\mu_{il} = \frac{1}{2} c^+_{il\sigma} \tau^\mu_{\sigma\sigma'} c_{il\sigma'} = \frac{1}{2} O_i{}^{\mu\nu} \Psi^+_{il\sigma} \tau^\nu_{\sigma\sigma'} \Psi_{il\sigma'}, \tag{2.10}$$

where

$$O_i{}^{\mu\nu} = \frac{1}{2} \text{Tr} g^+_i \tau^\mu g_i \tau^\nu. \tag{2.11}$$

It is convenient to introduce three basic vectors which depend on the Schwinger bosons

$$T^1_{i\mu} = O_i{}^{\mu 1}, \quad T^2_{i\mu} = O_i{}^{\mu 2}, \quad T^3_{i\mu} = O_i{}^{\mu 3}, \tag{2.12}$$

where $\mathbf{T}^3_i = \frac{1}{s}\mathbf{S}_i$. Then, the spin of the electrons can be represented as a linear combination of three vectors $\mathbf{S}_j$, $\mathbf{P}_j = \mathbf{T}^1_j + i\mathbf{T}^2_j$, and $\mathbf{P}^+_j = \mathbf{T}^1_j - i\mathbf{T}^2_j$

$$\mathbf{s}_{il} = \frac{1}{2s} \mathbf{S}_i (\Psi^{A+}_{il} \Psi^A_{il} - \Psi^{B+}_{il} \Psi^B_{il}) + \frac{1}{2} \mathbf{P}_i \Psi^{B+}_{il} \Psi^A_{il} + \frac{1}{2} \mathbf{P}^+_i \Psi^{A+}_{il} \Psi^B_{il}. \tag{2.13}$$

The basic vectors satisfy the relations $\mathbf{S}^2_i = s^2$, $\mathbf{P}^2_i = \mathbf{P}^{+2}_i = \mathbf{S}_i \cdot \mathbf{P}_i = \mathbf{S}_i \cdot \mathbf{P}^+_i = 0$, and $\mathbf{P}^+_i \cdot \mathbf{P}_i = 2$. Using the expression (2.13) for the spin of itinerant electrons, the total spin of the system

$$\mathbf{S}^{\text{tot}}_i = \mathbf{S}_i + \mathbf{s}_{i1} + \mathbf{s}_{i2} \tag{2.14}$$

can be written in the form

$$\mathbf{S}_i^{\mathrm{tot}} = \frac{1}{s}\left[s + \frac{1}{2}\sum_l (\Psi_{il}^{A+}\Psi_{il}^{A} - \Psi_{il}^{B+}\Psi_{il}^{B}) \right]\mathbf{S}_i + \frac{1}{2}\mathbf{P}_i\sum_l \Psi_{il}^{B+}\Psi_{il}^{A} + \frac{1}{2}\mathbf{P}_i^{+}\sum_l \Psi_{il}^{A+}\Psi_{il}^{B}. \tag{2.15}$$

The gauge invariance imposes the conditions $\langle \Psi_{il}^{A} + \Psi_{il}^{B}\rangle = \langle \Psi_{il}^{B} + \Psi_{il}^{A}\rangle = 0$. As a result, the dimensionless magnetization per lattice site $\langle (S_i^{\mathrm{tot}})^z\rangle$ reads

$$\langle (S_i^{\mathrm{tot}})^z\rangle = \frac{1}{s}\left[s + \frac{1}{2}\sum_l \langle (\Psi_{il}^{A+}\Psi_{il}^{A} - \Psi_{il}^{B+}\Psi_{il}^{B})\rangle \right]\langle \mathbf{S}_i^z\rangle. \tag{2.16}$$

Let us average the total spin of the system [Eq. (2.15)] in the subspace of the itinerant electrons $\langle \mathbf{S}_i^{\mathrm{tot}}\rangle_f = \mathbf{M}_i$. The vector $\mathbf{M}_i$ identifies the local orientation of the total magnetization. Accounting for the gauge invariance, one obtains the following expression for $\mathbf{M}_i$:

$$\langle \mathbf{S}_i^{\mathrm{tot}}\rangle_f = \mathbf{M}_i = \frac{M}{s}\mathbf{S}_i, \tag{2.17}$$

where

$$M = s + \frac{1}{2}\sum_l \langle (\Psi_{il}^{A+}\Psi_{il}^{A} - \Psi_{il}^{B+}\Psi_{il}^{B})\rangle \tag{2.18}$$

can be thought of as an "effective spin" of the system ($\mathbf{M}_i^2 = M^2$). Now, if we use Holstein-Primakoff representation for the vectors $\mathbf{M}_j$

$$M_j^{+} = M_{j1} + iM_{j2} = \sqrt{2M - a_j^{+}a_j}\,a_j,$$

$$M_j^{-} = M_{j1} - iM_{j2} = a_j^{+}\sqrt{2M - a_j^{+}a_j},$$

$$M_j^{3} = M - a_j^{+}a_j \tag{2.19}$$

the Bose fields a_j and a_j^{+} are the true magnons in the system. In terms of the true magnons the Schwinger bosons (2.2) have the following representation:

$$\varphi_{i1} = \sqrt{2s - \frac{s}{M}a_i^{+}a_i}, \quad \varphi_{i2} = \sqrt{\frac{s}{M}}a_i. \tag{2.20}$$

Replacing in Eqs. (2.5) and (2.6) for the spin-singlet Fermions and keeping only the first two terms in $1/M$ expansion $\sqrt{1-1/2M\,a_i^{+}a_i} \simeq 1 - \frac{1}{4M}a_i^{+}a_i + \cdots$ we obtain

$$\Psi_{il}^{A} = c_{il1} + \frac{1}{\sqrt{2M}}a_i^{+}c_{il2} - \frac{1}{4M}a_i^{+}a_i c_{il1} + \cdots, \tag{2.21}$$

$$\Psi_{il}^{B} = c_{il2} - \frac{1}{\sqrt{2M}}a_i c_{il1} - \frac{1}{4M}a_i^{+}a_i c_{il2} + \cdots. \tag{2.22}$$

The equations (2.21) and (2.22) show that the singlet fermions are electrons dressed by a virtual cloud of repeatedly emitted and reabsorbed magnons.

An important advantage of working with A and B fermions is the fact that in terms of these spin-singlet fields the spin-fermion interaction is in a diagonal form, the spin variables (magnons) are removed, and one accounts for it exactly:

$$\sum_{il} \vec{S}_i \cdot \vec{s}_{il} = \frac{s}{2}\sum_{il} (\Psi_{il}^{+A}\Psi_{il}^{A} - \Psi_{il}^{+B}\Psi_{il}^{B}). \tag{2.23}$$

Replacing all this into the action (2.4), we can rewrite it as a function of the Schwinger bosons and spin-singlet fermions. The resulting action is quadratic with respect to the spin-singlet fermions and one can integrate them out. The effective Hamiltonian of the theory, in Gaussian approximation, is given by

$$h_{\mathrm{eff}} = \rho\sum_{\langle ij\rangle} (a_i^{+}a_i + a_j^{+}a_j - a_i^{+}a_j - a_j^{+}a_i), \tag{2.24}$$

where ρ is the spin stiffness (A42). Detailed calculation are given in the appendix. Based on the rotational symmetry, one can supplement the Hamiltonian (Eq. (2.24)) up to an effective Heisenberg-like Hamiltonian, written in terms of the vectors $\mathbf{M}_i$

$$h_{\mathrm{eff}} = -J\sum_{\langle ij\rangle} \mathbf{M}_i \cdot \mathbf{M}_j, \tag{2.25}$$

where $J = \rho/M$. The ferromagnetic phase is stable if the effective exchange coupling constant is positive $J > 0$.

It is important to highlight the difference between the above effective theory (2.25) and Ruderman-Kittel-Kasuya-Yosida (RKKY) theory. The RKKY effective Hamiltonian is an effective Heisenberg-like Hamiltonian in terms of core spins $\mathbf{S}_i$, obtained averaging in the subspace of the itinerant electrons.[8] The subtle point is that if we use a Holstein-Primakoff representation for the localized spins $\mathbf{S}_i$, the creation and annihilation bose operators do not describe the true magnon of the system.[18,19] The true magnons are transversal fluctuations corresponding to the total magnetization which includes both the spins of localized and delocalized electrons. Therefore the RKKY validity condition requires small Hund's coupling, and small density of charge carriers, which in turn means that the magnetization of the mobile electrons is inessential. In contrast of RKKY theory the effective model (2.25) is written in term of vectors $\mathbf{M}_i$ which describe the local orientations of the total magnetization, and the bose operators in Eq. (2.19) are the true magnons in the theory. This is essential when one calculates the Curie temperature. The effective model (2.25) is obtained integrating out the spin-singlet fermions (2.5) and (2.6). In terms of these fermions the Hund's interaction is in a diagonal form and we account for it exactly. Hence, the effective theory (2.25) is valid for arbitrary values of Hund's constants and for all densities of charge carriers.

III. PHASE DIAGRAMS

Here we illustrate some of the features of our model, namely, the phase diagrams and how they change when we vary the model's parameters. Since calculating T_c is closely related to calculating spin stiffness ρ, we have examined the behavior of ρ as a function of electron density in details.

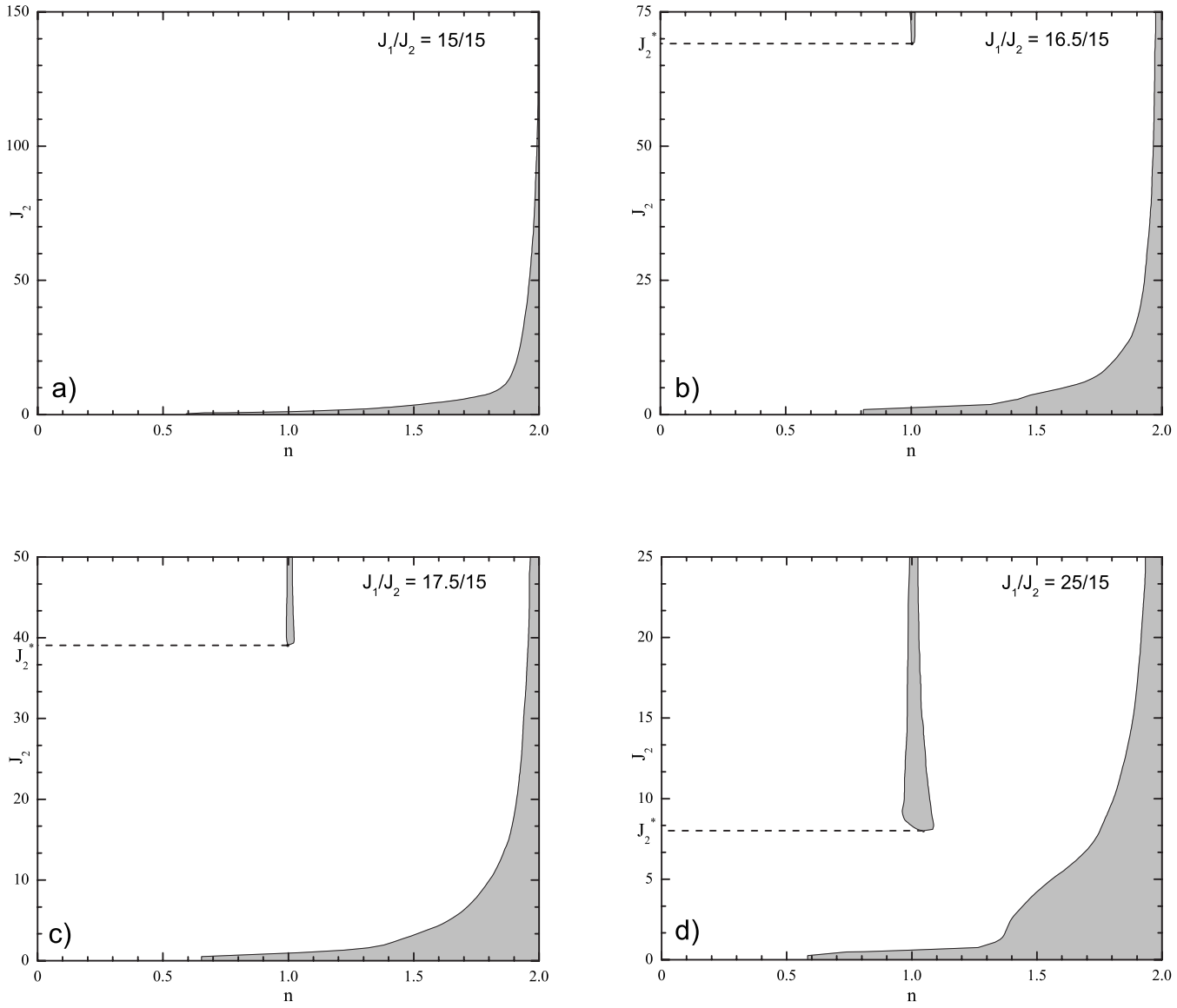

FIG. 1. Phase diagrams for the four cases under consideration at $t'=0.5$: (a) $J_1/J_2=1$, (b) $J_1/J_2=16.5/15$, (c) $J_1/J_2=17.5/15$, and (d) $J_1/J_2=25/15$. White regions correspond to FM phase, grayed ones to FM instability.

The physics of the model depends on dimensionless parameters J_1/t_1, J_2/t_1, t_2/t_1, and t'/t_1. Throughout this chapter we fix the scale setting $t_1=t_2=1$, and use J_1, J_2, and t' as a free parameters of the model. Also in this section $t'=0.5$, and since we are describing manganite materials, we have set $s=3/2$. The phase diagrams in Fig. 1 are constructed by plotting the curve $\rho=0$ in coordinate system of carrier density n and J_2/t_1 for fixed ratio J_1/J_2. Regions where $\rho>0$ correspond to the ferromagnetic phase (FM), while those with $\rho<0$ are denoted here simply as non-FM ones, since describing all possible phases is not the purpose of this paper.

We consider four different cases for the ratio J_1/J_2, namely, $J_1/J_2=15/15$, where the bands are degenerated, and three cases with increasing bands' splitting $J_1/J_2=16.5/15$, $J_1/J_2=17.5/15$ and $J_1/J_2=25/15$. The values of those ratios are chosen to compare our model with available results.[15]

When the bands are split, we observe an island of ferromagnetic instability around the line $n=1$. The lowest point of the island is denoted by J_2^*. Increasing the ratio J_1/J_2 increases the island by lowering the value of J_2^* (see Fig. 1). This is a new aspect of the two-band situation compared to the single-band one. For the degenerated bands ($J_1/J_2=1$), we have not observed the island of ferromagnetic instability, up to values as large as $J_2=300$, and the boundary curve resembles the one in the single-band model.

The value of the spin stiffness constant ρ depends on the point (n,J_2) in the phase diagram, for fixed ratio J_1/J_2. When the point approaches the boundary of the ferromagnetic phase, the value of ρ decreases and reaches zero on the boundary (by the definition of the boundary). We have calculated the spin stiffness constant ρ as a function of n, for fixed J_2 at zero temperature. There are three distinctive cases: $J_2>J_2^*$, $J_2\lesssim J_2^*$ and $J_2\ll J_2^*$.

For the first one, the presence of ferromagnetic instability near $n=1$ results in a function $\rho(n)$, which consists of two pieces, one for n in the interval (0, 1), and another for n in

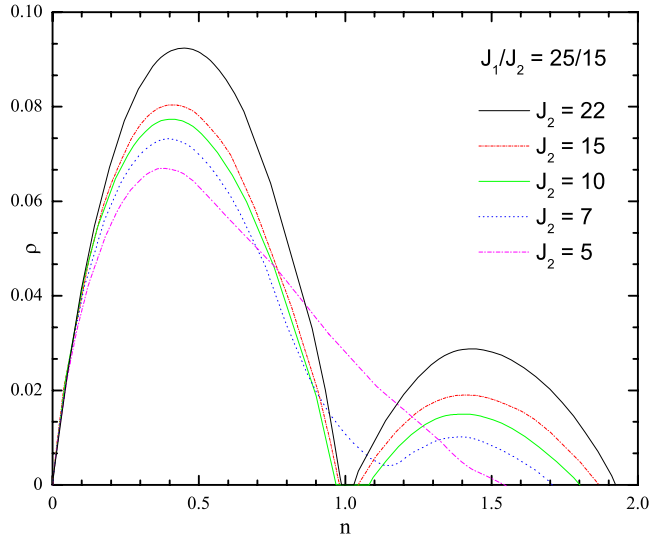

FIG. 2. (Color online) ρ as a function of n for the forth case $J_1/J_2=25/15$, corresponding to Fig. 1(d).

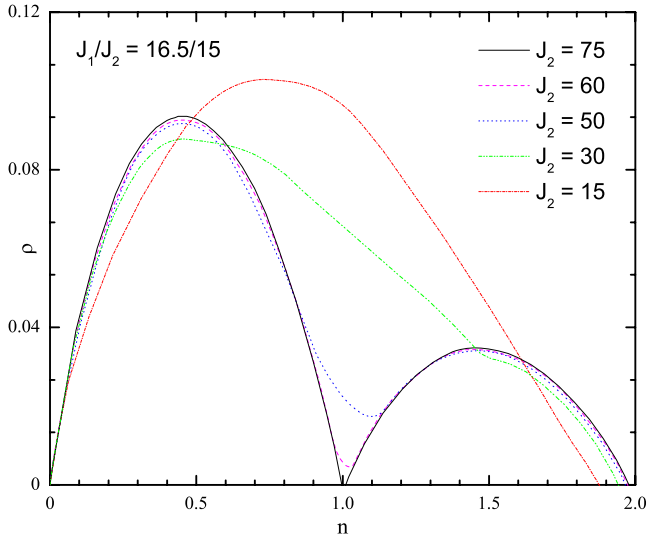

FIG. 4. (Color online) ρ as a function of n for the second case $J_1/J_2=16.5/15$, corresponding to Fig. 1(b).

the interval (1,2). For the ratio $J_1/J_2=25/15$ (Fig. 2), such are the curves corresponding to $J_2=22$, $J_2=15$ and $J_2=10$; for $J_1/J_2=17.5/15$ (Fig. 3) the curve corresponding to $J_2=45$; and for $J_1/J_2=16.5/15$ (Fig. 4) the one corresponding to $J_2=75$. The important characteristic of all these curves is the existence of two maxima, one within interval $(0,1)$, and another one within interval $(1,2)$. The global maximum is within the interval (0,1), which is result of the presence of two phase boundaries in the other interval. In the case of degenerated bands, the absence of island of instability leads to the absence of such type of function $\rho(n)$.

For the second one, J_2 is very close to J_2^*, hence near $n=1$ the spin stiffness constant is very small. As a result $\rho(n)$ is a function with two maxima and one minimum. For the ratio $J_1/J_2=25/15$ (Fig. 2), such is the curve corresponding to $J_2=7$; for $J_1/J_2=17.5/15$ (Fig. 3) the curves corresponding to $J_2=30$ and $J_2=25$; and for $J_1/J_2=16.5/15$ (Fig. 4) the ones corresponding to $J_2=60$ and $J_2=50$. The minimal value of the function decreases when J_2 approaches J_2^*. Again, in the special case of degenerated bands, there is no such a curve.

For the third case, $J_2 \ll J_2^*$, we are well below the island of ferromagnetic instability, and the function $\rho(n)$ has only one maximum within the interval (0,1). For the ratio $J_1/J_2=25/15$ (Fig. 2), such is the curve corresponding to $J_2=5$; for $J_1/J_2=17.5/15$ (Fig. 3) the curves corresponding to $J_2=20$ and $J_2=15$; and for $J_1/J_2=16.5/15$ (Fig. 4) the ones corresponding to $J_2=30$ and $J_2=15$. In the case of degenerated bands, for all values of J_2 the curves are of this type because of the absence of instability island (Fig. 5).

It is a widely known fact that near $n=2$ the system is ferromagnetically unstable and the spin stiffness constant ap-

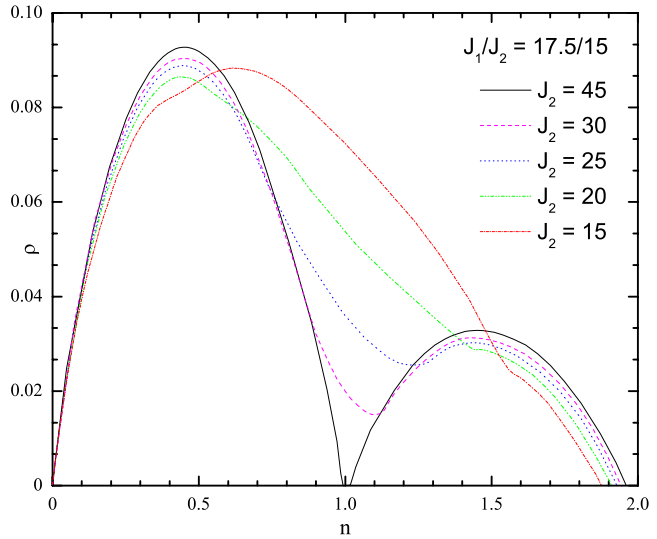

FIG. 3. (Color online) ρ as a function of n for the third case $J_1/J_2=17.5/15$, corresponding to Fig. 1(c).

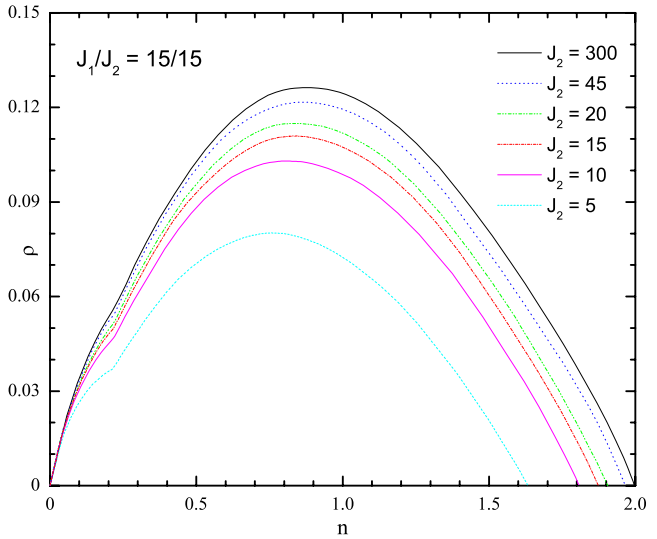

FIG. 5. (Color online) ρ as a function of n for the degenerated case $J_1/J_2=15/15$, corresponding to Fig. 1(a).

proaches zero when the carrier density approaches 2. One can see from the phase diagrams (Fig. 1), that with decreasing J_2, ferromagnetic instability sets in for smaller values of n. As a result we obtain that with decreasing J_2, the value of n for which $\rho(n)=0$ decreases. This is best observed in the case of degenerated bands, where we have examined broader set of values for J_2. With increasing of J_2, the point $\rho=0$ gets closer to $n=2$ and the curve becomes more symmetric.

For all four ratios we have performed calculations for $J_2=15$ (red lines in the figures), to compare our results with the results in Ref. 15. Since the maximum value of the Curie temperature corresponds to the maximum value of the spin stiffness constant, it is important to see how this value depends on the ratio J_1/J_2 for fixed J_2. Increasing J_1/J_2 increases the ferromagnetic instability (see phase portraits Fig. 1), lowering the point J_2^* which in turn leads to decrease of the maximum value of ρ and qualitative changes in its behavior as a function of density n.

IV. CURIE TEMPERATURES

To calculate the Curie temperature we utilize the Schwinger-bosons mean-field theory.[21,22] The advantage of this method of calculation is that for 2D systems one obtains zero Curie temperature, in accordance with the Mermin-Wagner theorem.[17] So, while approximate, this technique of calculation captures the essentials of the magnon fluctuations in the theory.

To proceed, we represent the effective spin vector $\mathbf{M}_i$ by means of Schwinger bosons $\phi_{i\sigma}, \phi_{i\sigma}^+$,

$$M_i^\nu = \frac{1}{2}\sum_{\sigma\sigma'} \phi_{i\sigma}^+ \tau_{\sigma\sigma'}^\nu \phi_{i\sigma'}, \quad \phi_{i\sigma}^+\phi_{i\sigma} = 2M. \tag{4.1}$$

Next we use the identity

$$\mathbf{M}_i \cdot \mathbf{M}_j = \frac{1}{2}(\phi_{i\sigma}^+\phi_{j\sigma})(\phi_{j\sigma'}^+\phi_{i\sigma'}) - \frac{1}{4}(\phi_{i\sigma}^+\phi_{i\sigma})(\phi_{j\sigma'}^+\phi_{j\sigma'}) \tag{4.2}$$

and rewrite the effective Hamiltonian in the form

$$h_{\text{eff}} = -\frac{J}{2}\sum_{\langle ij\rangle} (\phi_{i\sigma}^+\phi_{j\sigma})(\phi_{j\sigma'}^+\phi_{i\sigma'}), \tag{4.3}$$

where the second term in Eq. (4.2) is equal to the constant M^2, because of the constraint (4.1), and we drop it. To ensure the constraint (4.1) we introduce a parameter (λ) and add a new term to the effective Hamiltonian (4.3)

$$\hat{h}_{\text{eff}} = h_{\text{eff}} + \lambda\sum_i (\phi_{i\sigma}^+\phi_{i\sigma} - 2M). \tag{4.4}$$

We treat the four-boson interaction within Hartree-Fock approximation. The Hartree-Fock Hamiltonian which corresponds to the effective Hamiltonian (4.4) reads

$$h_{\text{HF}} = \frac{J}{2}\sum_{\langle ij\rangle} \bar{u}_{ij}u_{ij} - \frac{J}{2}\sum_{\langle ij\rangle} [\bar{u}_{ij}\phi_{i\sigma}^+\phi_{j\sigma} + u_{ij}\phi_{j\sigma}^+\phi_{i\sigma}] + \lambda\sum_i (\phi_{i\sigma}^+\phi_{i\sigma} - 2M), \tag{4.5}$$

where $\bar{u}_{ij}(u_{ij})$ are Hartree-Fock parameters to be determined self-consistently. We are interested in real parameters which do not depend on the lattice sites, $u_{ij}=\bar{u}_{ij}=u$. Then in momentum space representation, the Hamiltonian (4.5) has the form

$$h_{\text{HF}} = \frac{3J}{2}Nu^2 - 2\lambda MN + \sum_k \varepsilon_k \phi_k^+\phi_k, \tag{4.6}$$

where N is the number of lattice sites and

$$\varepsilon_k = \lambda - Ju(\cos k_x + \cos k_y + \cos k_z) \tag{4.7}$$

is the dispersion of the ϕ_k boson (spinon).

The free energy of a theory with Hamiltonian (4.6) is

$$F = \frac{3J}{2}u^2 - 2\lambda M + \frac{2T}{N}\sum_k \ln(1 - e^{-\varepsilon_k/T}), \tag{4.8}$$

where T is the temperature. The self-consistent equations for parameters u and λ are

$$\frac{\partial F}{\partial u} = 0, \quad \frac{\partial F}{\partial \lambda} = 0. \tag{4.9}$$

We obtain a system of two equations

$$u = \frac{2}{3}\frac{1}{N}\sum_k n_k(\cos k_x + \cos k_y + \cos k_z), \tag{4.10}$$

$$M = \frac{1}{N}\sum_k n_k, \tag{4.11}$$

where n_k is the bose function

$$n_k = \frac{1}{e^{\varepsilon_k/T} - 1}. \tag{4.12}$$

To ensure correct definition of the bose theory (4.6), i.e., $\varepsilon_k \geqslant 0$ when the wave vector k runs over the first Brillouin zone of a cubic lattice, we have to make some assumptions for the parameter λ. For that purpose it is convenient to represent it in the form

$$\lambda = 3Ju + \mu Ju. \tag{4.13}$$

In terms of the new parameter μ, the Bose dispersion is

$$\varepsilon_k = Ju(3 - \cos k_x - \cos k_y - \cos k_z + \mu) \tag{4.14}$$

and the theory is well defined for $\mu \geqslant 0$.

We find the parameters μ and u solving Eqs. (4.10) and (4.11). For high enough temperatures both $\mu(T)>0$ and $u(T)>0$ and the excitation is gapped. It is the spinon excitation in the theory in the paramagntic phase. Decreasing the temperature leads to decrease of $\mu(T)$. At temperature T_C it becomes equal to zero and long-range excitation emerges in the spectrum. Hence the temperature at witch μ reaches zero

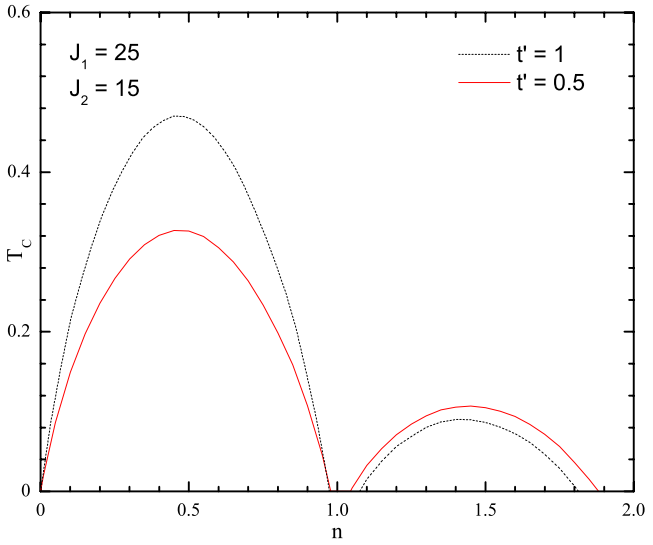

FIG. 6. (Color online) Curie temperature T_C as a function of charge density n for $J_1=25$, $J_2=15$, with $t'=1/2$ and $t'=1$.

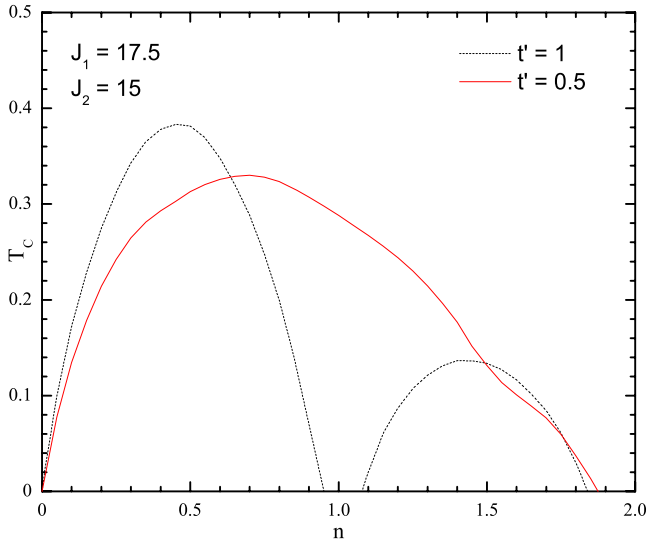

FIG. 7. (Color online) Curie temperature T_C as a function of charge density n for $J_1=17.5$, $J_2=15$, with $t'=1/2$ and $t'=1$.

is the Curie temperature. We set $\mu=0$ in the system of equations (4.10) and (4.11) and obtain a system of two equations for the Curie temperature T_C and the parameter u, which is the renormalization of the exchange constant at Curie temperature

$$u=\frac{2}{3}\frac{1}{N}\sum_k \frac{\cos k_x+\cos k_y+\cos k_z}{e^{(\rho u/MT_C)(3-\cos k_x-\cos k_y-\cos k_z)}-1},$$

$$M=\frac{1}{N}\sum_k \frac{1}{e^{(\rho u/MT_C)(3-\cos k_x-\cos k_y-\cos k_z)}-1}. \quad (4.15)$$

To calculate T_C we solve the above system of equations, with $M(T)$ and $\rho(T)$ calculated from Eqs. (2.18) and (A42), respectively.

The results for the Curie temperature T_C as a function of charge density n are plotted in Figs. 6–9, for two different values of interband hopping parameter t'. In all cases we have set $t_1=t_2=1$, and consider a theory with $s=3/2$ for the core spins. We want to compare our results with the results in Ref. 15, so we have calculated T_C for $J_2=15$ and $t'=0.5$ as well (red curves). Since our method of calculating T_C involves $\rho(T)$, the resulting curves are very similar to the ones in Sec. III (Figs. 2–5), and bear their characteristics. As above we have three different choices for the parameters $J_2>J_2^*$, $J_2\lesssim J_2^*$, and $J_2\ll J_2^*$. For the biggest ratio we consider $J_1/J_2=25/15$ (see Fig. 6), we have a two-piece function, since our chosen value $J_2>J_2^*$. With decreasing the ratio, the point J_2^* moves to higher values and J_2 becomes smaller than J_2^*. As a result the curves we obtained have only one maximum. It is important to note that even for the degenerated case $J_1/J_2=1$, the point at which T_C reaches zero is smaller than $n=2$ unlike the results in Ref. 15. This can be also seen from the phase portraits (Fig. 1), where the instability of ferromagnetism near the charge carriers density $n=2$ is evident. One can also note that for $t'=1$ decreasing the ratio J_1/J_2 leads to increase in the maximum value of $T_C(n)$, while when $t'=0.5$ the $T_C(n)$ is maximal when $J_1=J_2$. Similar result was found in a two-band model applied to dilute systems.[22]

The most important difference between our curves of critical temperature as a function of n and the ones in Ref. 15 is the lack of symmetry with respect to $n=1$. This asymmetry originates from asymmetry in the phase diagrams, which in turn leads to asymmetry of the spin-stiffness curves. The two-peak structure of $T_C(n)$ in Fig. 6 is a consequence of the fact that the bands occupy different energy intervals (very different couplings). The asymmetry diminishes when the partial overlap of the bands increases (the values of $J's$ are close, see Figs. 7 and 8), and the form of the $T_C(n)$ curve becomes approximately semicircular (see Fig. 9) when the overlap is maximal ($J_1=J_2$). At $t'=0.5$ the curve in Fig. 9 resembles the result in Ref. 15.

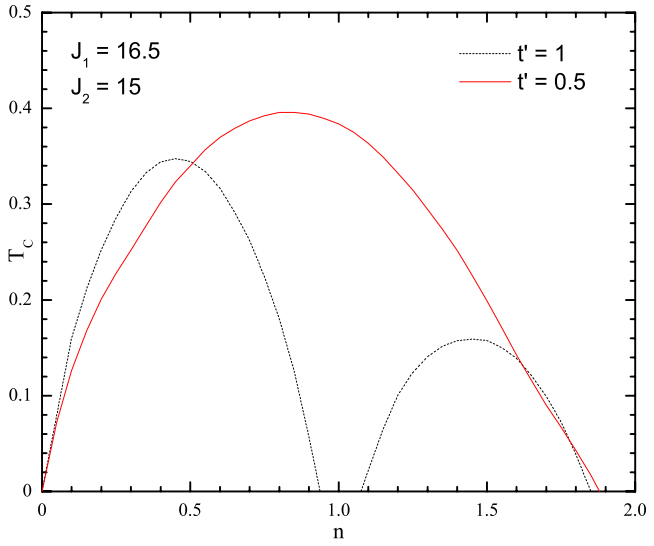

FIG. 8. (Color online) Curie temperature T_C as a function of charge density n for $J_1=16.5$, $J_2=15$, with $t'=1/2$ and $t'=1$.

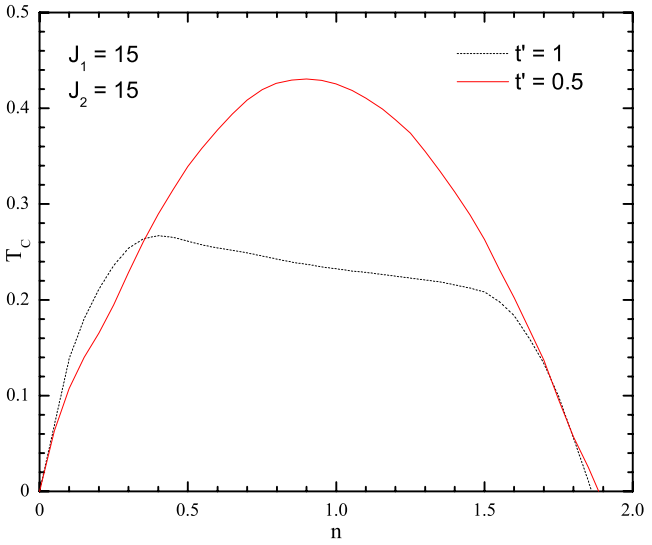

FIG. 9. (Color online) Curie temperature T_C as a function of charge density n for the degenerated case $J_1=15$, $J_2=15$, with $t'=1/2$ and $t'=1$.

We have also examined the effect of t'. Increasing its value results in enlargement of the ferromagnetic instability island around $n=1$. The value of J_2^* decreases and the width of the island increases. This in turn leads to both quantitative and qualitative changes in $T_C(n)$ (see the black lines of Figs. 6–9). An important conclusion is that Curie temperature increases with increasing t' if the bands are strongly split (very different J couplings, Figs. 6 and 7), while for weakly split bands $(J_1/J_2 \gtrsim 1)$, we obtained an opposite behavior, the critical temperature decreases (Figs. 8 and 9).

V. SUMMARY

In summary, we have calculated the Curie temperature in two-band double exchange model. First we reduced the model to an effective Heisenberg-type model for a vector which describes the local orientations of the total magnetization. Next, we use Schwinger-bosons mean-field theory to calculate the critical temperature. This technique of calculation is in agreement with Mermin-Wagner theorem, which means that employing our method of calculations for 2D system one obtains $T_C=0$.[20,21]

There are many quantitative and qualitative differences between our results and the results obtained within dynamical mean-field theory or Monte Carlo simulation approach. Maybe the most significant difference is that DMFT and MC calculations lead to temperature's curves, as a function of fermion density, symmetric with respect to $n=1$. This is not the result in the present paper. The asymmetry of the $T_C(n)$ curves with respect to $n=1$ is a characteristic feature in our approach. This asymmetry is seen looking at the phase diagrams. It predetermines the asymmetry of the spin-stiffness curves which lead directly to the asymmetric $T_C(n)$ curves. The symmetry mentioned in the paper Ref. 15 is possible if the two bands are degenerated and Hund's constants are unphysically large.

Another important result reported in previous papers is that the critical temperature increases with increasing the interband hopping. Our calculations show that this is true when the band splitting is strong. If the bands split weakly, the assertion is opposite. The Curie temperature increases when the interband hopping decreases.

ACKNOWLEDGMENTS

The authors acknowledge the financial support of the Sofia University, Project No. 037/2007.

APPENDIX: CALCULATION OF ρ

Here we present a detailed derivation of the spin stiffness constant ρ. We start from the two-band Hamiltonian (2.1) and rewrite it in terms of Scwinger bosons (2.2) and spin-singlet fermions (2.5) and (2.6).

The resulting action is quadratic with respect to the spin-singlet fermions and one can integrate them out. To do so, it is convenient to represent the action as a sum of three terms

$$S = S_f + S_{s\text{-}f}^{(1)} + S_{s\text{-}f}^{(2)}, \tag{A1}$$

where S_f is the free fermion action

$$S_f = \int_0^\beta d\tau \left\{ \sum_{i\sigma} \left(\Psi_{i1\sigma}^+ \frac{\partial}{\partial\tau} \Psi_{i1\sigma} + \Psi_{i2\sigma}^+ \frac{\partial}{\partial\tau} \Psi_{i2\sigma} \right) + H_f \right\} \tag{A2}$$

with free fermion Hamiltonian H_f

$$\begin{aligned} H_f = & -s \sum_{il} J_l (\Psi_{il}^{+A} \Psi_{il}^A - \Psi_{il}^{+B} \Psi_{il}^B) - \mu \sum_{il\sigma} \Psi_{il\sigma}^+ \Psi_{il\sigma} \\ & - \sum_{\langle ij\rangle\sigma} t_1 (\Psi_{i1\sigma}^+ \Psi_{j1\sigma} + \Psi_{j1\sigma}^+ \Psi_{i1\sigma}) - \sum_{\langle ij\rangle\sigma} t_2 (\Psi_{i2\sigma}^+ \Psi_{j2\sigma} \\ & + \Psi_{j2\sigma}^+ \Psi_{i2\sigma}) - \sum_{\langle ij\rangle\sigma} t' (\Psi_{i1\sigma}^+ \Psi_{j2\sigma} + \Psi_{j2\sigma}^+ \Psi_{i1\sigma} + \Psi_{i2\sigma}^+ \Psi_{j1\sigma} \\ & + \Psi_{j1\sigma}^+ \Psi_{i2\sigma}). \end{aligned} \tag{A3}$$

We remind the reader of the notations $\Psi_{il1}=\Psi_{il}^A$ and $\Psi_{il2}=\Psi_{il}^B$, so that the sum over σ in the above equation is a sum over A and B. It is convenient to represent the term describing spin-fermion interaction as a sum of two terms

$$\begin{aligned} S_{s\text{-}f}^{(1)} = & \int_0^\beta d\tau \left\{ -\frac{t_1}{2s} \sum_{\langle ij\rangle} [(\varphi_{i\sigma}^+ \varphi_{j\sigma} - 2s)(\Psi_{1i}^{+A} \Psi_{1j}^A + \Psi_{1j}^{+B} \Psi_{1i}^B) \right. \\ & + (\varphi_{j\sigma}^+ \varphi_{i\sigma} - 2s)(\Psi_{1i}^{+B} \Psi_{1j}^B + \Psi_{1j}^{+A} \Psi_{1i}^A)] - \frac{t_2}{2s} \sum_{\langle ij\rangle} [(\varphi_{i\sigma}^+ \varphi_{j\sigma} \\ & - 2s)(\Psi_{2i}^{+A} \Psi_{2j}^A + \Psi_{2j}^{+B} \Psi_{2i}^B) + (\varphi_{j\sigma}^+ \varphi_{i\sigma} - 2s)(\Psi_{2i}^{+B} \Psi_{2j}^B \\ & + \Psi_{2j}^{+A} \Psi_{2i}^A)] - \frac{t'}{2s} \sum_{\langle ij\rangle} [(\varphi_{i\sigma}^+ \varphi_{j\sigma} - 2s)(\Psi_{1i}^{+A} \Psi_{2j}^A + \Psi_{2i}^{+A} \Psi_{1j}^A \\ & + \Psi_{2j}^{+B} \Psi_{1i}^B + \Psi_{1j}^{+B} \Psi_{2i}^B) + (\varphi_{j\sigma}^+ \varphi_{i\sigma} - 2s)(\Psi_{1i}^{+B} \Psi_{2j}^B \\ & \left. + \Psi_{2i}^{+B} \Psi_{1j}^B + \Psi_{2j}^{+A} \Psi_{1i}^A + \Psi_{1j}^{+A} \Psi_{2i}^A)] \right\}, \end{aligned} \tag{A4}$$

$$S_{s\text{-}f}^{(2)} = \int_0^\beta d\tau \Bigg\{ -\frac{t_1}{2s}\sum_{\langle ij\rangle}[(\varphi_{i1}^+\varphi_{j2}^+ - \varphi_{j1}^+\varphi_{i2}^+)(\Psi_{1j}^{+A}\Psi_{1i}^B - \Psi_{1i}^{+A}\Psi_{1j}^B) + (\varphi_{i1}\varphi_{j2} - \varphi_{i2}\varphi_{j1})(\Psi_{1i}^{+B}\Psi_{1j}^A - \Psi_{1j}^{+B}\Psi_{1i}^A)] - \frac{t_2}{2s}\sum_{\langle ij\rangle}[(\varphi_{i1}^+\varphi_{j2}^+ - \varphi_{j1}^+\varphi_{i2}^+)(\Psi_{2j}^{+A}\Psi_{2i}^B - \Psi_{2i}^{+A}\Psi_{2j}^B) + (\varphi_{i1}\varphi_{j2} - \varphi_{i2}\varphi_{j1})(\Psi_{2i}^{+B}\Psi_{2j}^A - \Psi_{2j}^{+B}\Psi_{2i}^A)] - \frac{t'}{2s}\sum_{\langle ij\rangle}[(\varphi_{i1}^+\varphi_{j2}^+ - \varphi_{j1}^+\varphi_{i2}^+)(\Psi_{1j}^{+A}\Psi_{2i}^B + \Psi_{2j}^{+A}\Psi_{1i}^B - \Psi_{1i}^{+A}\Psi_{2j}^B - \Psi_{2i}^{+A}\Psi_{1j}^B) + (\varphi_{i1}\varphi_{j2} - \varphi_{i2}\varphi_{j1})(\Psi_{2i}^{+B}\Psi_{1j}^A + \Psi_{1i}^{+B}\Psi_{2j}^A - \Psi_{1j}^{+B}\Psi_{2i}^A - \Psi_{2j}^{+B}\Psi_{1i}^A)] \Bigg\}. \tag{A5}$$

To diagonalize the free fermion Hamiltonian H_f we switch to momentum space

$$H_f = \sum_{lk}[\varepsilon_{kl}^A \Psi_{lk}^{A+}\Psi_{lk}^A + \varepsilon_{kl}^B \Psi_{lk}^{B+}\Psi_{lk}^B] + \sum_{k\sigma}[\varepsilon_k(\Psi_{1k\sigma}^+\Psi_{2k\sigma} + \Psi_{2k\sigma}^+\Psi_{1k\sigma})], \tag{A6}$$

where the dispersions for A and B fermions are

$$\varepsilon_{kl}^A = -2t_l\sum_k \cos k_\mu - sJ_l - \mu,$$

$$\varepsilon_{kl}^B = -2t_l\sum_k \cos k_\mu + sJ_l - \mu,$$

$$\varepsilon(k) = -2t'\sum_\mu \cos k_\mu. \tag{A7}$$

The Hamiltonian is diagonalized by means of the transformation

$$\Psi_{1k}^A = u_k^A f_{1k}^A + v_k^A f_{2k}^A, \quad \Psi_{2k}^A = -v_k^A f_{1k}^A + u_k^A f_{2k}^A,$$

$$\Psi_{1k}^B = u_k^B f_{1k}^B + v_k^B f_{2k}^B, \quad \Psi_{2k}^B = -v_k^B f_{1k}^B + u_k^B f_{2k}^B. \tag{A8}$$

Solving the equations for u and v gives

$$u_k^R = \sqrt{\frac{1}{2}(1 + x_k^R)},$$

$$v_k^R = \mathrm{sgn}[\varepsilon(k)]\sqrt{\frac{1}{2}(1 - x_k^R)} \tag{A9}$$

$$\text{with } x_k^R = \frac{\varepsilon_{2k}^R - \varepsilon_{1k}^R}{\sqrt{4\varepsilon^2(k) + (\varepsilon_{2k}^R - \varepsilon_{1k}^R)^2}}. \tag{A10}$$

The resulting Hamiltonian is

$$H_f = \sum_k [E_{1k}^A f_{1k}^{+A} f_{1k}^A + E_{1k}^B f_{1k}^{+B} f_{1k}^B + E_{2k}^A f_{2k}^{+A} f_{2k}^A + E_{2k}^B f_{2k}^{+B} f_{2k}^B] \tag{A11}$$

with dispersions for the quasiparticles

$$E_{1k}^A = \frac{\varepsilon_{2k}^A + \varepsilon_{1k}^A}{2} - \frac{1}{2}\sqrt{4\varepsilon^2(k) + (\varepsilon_{2k}^A - \varepsilon_{1k}^A)^2},$$

$$E_{2k}^A = \frac{\varepsilon_{2k}^A + \varepsilon_{1k}^A}{2} + \frac{1}{2}\sqrt{4\varepsilon^2(k) + (\varepsilon_{2k}^A - \varepsilon_{1k}^A)^2}, \tag{A12}$$

$$E_{1k}^B = \frac{\varepsilon_{2k}^B + \varepsilon_{1k}^B}{2} - \frac{1}{2}\sqrt{4\varepsilon^2(k) + (\varepsilon_{2k}^B - \varepsilon_{1k}^B)^2},$$

$$E_{2k}^B = \frac{\varepsilon_{2k}^B + \varepsilon_{1k}^B}{2} + \frac{1}{2}\sqrt{4\varepsilon^2(k) + (\varepsilon_{2k}^B - \varepsilon_{1k}^B)^2}. \tag{A13}$$

To write the spin-fermion interaction $S_{s\text{-}f}$ in terms of the new fermions we introduce the notations

$$f_{k_1}^+ = (f_{1k_1}^{+A}\ f_{1k_1}^{+B}\ f_{2k_1}^{+A}\ f_{2k_1}^{+B}), \quad f_{k_2} = \begin{pmatrix} f_{1k_2}^A \\ f_{1k_2}^B \\ f_{2k_2}^A \\ f_{2k_2}^B \end{pmatrix}. \tag{A14}$$

Now we rewrite the action in the form

$$S_{s\text{-}f} = \int_0^\beta d\tau_1 d\tau_2 \sum_{k_1k_2} f_{k_1}^+(\tau_1) W_{k_1k_2}(\tau_1 - \tau_2) f_{k_2}(\tau_2), \tag{A15}$$

where the matrix $W_{k_1k_2}(\tau_1 - \tau_2)$ is a sum of two terms

$$W_{k_1k_2}(\tau_1 - \tau_2) = W_{k_1k_2}^0(\tau_1 - \tau_2) + W_{k_1k_2}^{\mathrm{int}}(\tau_1 - \tau_2). \tag{A16}$$

$W_{k_1k_2}^0(\tau_1 - \tau_2)$ is the free fermion action

$$W_{k_1k_2}^0(\tau_1 - \tau_2) = \delta_{k_1k_2}\delta(\tau_1 - \tau_2)\begin{pmatrix} \frac{\partial}{\partial\tau_2} + E_{1k_2}^A & 0 & 0 & 0 \\ 0 & \frac{\partial}{\partial\tau_2} + E_{1k_2}^B & 0 & 0 \\ 0 & 0 & \frac{\partial}{\partial\tau_2} + E_{2k_2}^A & 0 \\ 0 & 0 & 0 & \frac{\partial}{\partial\tau_2} + E_{2k_2}^B \end{pmatrix} \tag{A17}$$

while $W^{\text{int}}_{k_1k_2}(\tau_1-\tau_2)$ is a sum of two matrixes, corresponding to $S^{(1)}_{s\text{-}f}$ and $S^{(2)}_{s\text{-}f}$

$$W^{\text{int}}_{k_1k_2}(\tau_1-\tau_2)=\delta(\tau_1-\tau_2)\begin{pmatrix} K_{k_1k_2}(\tau_2) & 0 & 0 & 0\\ 0 & L_{k_1k_2}(\tau_2) & 0 & 0\\ 0 & 0 & N_{k_1k_2}(\tau_2) & 0\\ 0 & 0 & 0 & O_{k_1k_2}(\tau_2)\end{pmatrix}+\delta(\tau_1-\tau_2)\begin{pmatrix} 0 & A_{k_1k_2}(\tau_2) & 0 & B_{k_1k_2}(\tau_2)\\ C_{k_1k_2}(\tau_2) & 0 & D_{k_1k_2}(\tau_2) & 0\\ 0 & E_{k_1k_2}(\tau_2) & 0 & F_{k_1k_2}(\tau_2)\\ G_{k_1k_2}(\tau_2) & 0 & I_{k_1k_2}(\tau_2) & 0\end{pmatrix} \tag{A18}$$

with matrix elements

$$K_{k_1k_2}(\tau_2)=-\frac{1}{2s}\frac{1}{N}\sum_k\left(\sum_{\mu=1}^{3}\frac{\cos k_\mu}{3}\right)\sum_{\langle ij\rangle}(\varphi^+_{i\sigma}\varphi_{j\sigma}+\varphi^+_{j\sigma}\varphi_{i\sigma}-4s)[t_1(u^A_k)^2+t_2(v^A_k)^2-2t'u^A_kv^A_k],$$

$$L_{k_1k_2}(\tau_2)=-\frac{1}{2s}\frac{1}{N}\sum_k\left(\sum_{\mu=1}^{3}\frac{\cos k_\mu}{3}\right)\sum_{\langle ij\rangle}(\varphi^+_{i\sigma}\varphi_{j\sigma}+\varphi^+_{j\sigma}\varphi_{i\sigma}-4s)[t_1(u^B_k)^2+t_2(v^B_k)^2-2t'u^B_kv^B_k],$$

$$K_{k_1k_2}(\tau_2)=-\frac{1}{2s}\frac{1}{N}\sum_k\left(\sum_{\mu=1}^{3}\frac{\cos k_\mu}{3}\right)\sum_{\langle ij\rangle}(\varphi^+_{i\sigma}\varphi_{j\sigma}+\varphi^+_{j\sigma}\varphi_{i\sigma}-4s)[t_1(v^A_k)^2+t_2(u^A_k)^2+2t'u^A_kv^A_k],$$

$$L_{k_1k_2}(\tau_2)=-\frac{1}{2s}\frac{1}{N}\sum_k\left(\sum_{\mu=1}^{3}\frac{\cos k_\mu}{3}\right)\sum_{\langle ij\rangle}(\varphi^+_{i\sigma}\varphi_{j\sigma}+\varphi^+_{j\sigma}\varphi_{i\sigma}-4s)[t_1(v^B_k)^2+t_2(u^B_k)^2+2t'u^B_kv^B_k], \tag{A19}$$

$$A_{k_1k_2}(\tau_2)=-\frac{1}{2s}\frac{1}{N}\sum_{\langle ij\rangle}(\varphi^+_{i1}\varphi^+_{j2}-\varphi^+_{j1}\varphi^+_{i2})(e^{-ik_1r_j+ik_2r_i}-e^{-ik_1r_i+ik_2r_j})[t_1u^A_{k_1}u^B_{k_2}+t_2v^A_{k_1}v^B_{k_2}-t'u^A_{k_1}v^B_{k_2}-t'v^A_{k_1}u^B_{k_2}],$$

$$B_{k_1k_2}(\tau_2)=-\frac{1}{2s}\frac{1}{N}\sum_{\langle ij\rangle}(\varphi^+_{i1}\varphi^+_{j2}-\varphi^+_{j1}\varphi^+_{i2})(e^{-ik_1r_j+ik_2r_i}-e^{-ik_1r_i+ik_2r_j})[t_1u^A_{k_1}v^B_{k_2}-t_2v^A_{k_1}u^B_{k_2}+t'u^A_{k_1}u^B_{k_2}-t'v^A_{k_1}v^B_{k_2}],$$

$$E_{k_1k_2}(\tau_2)=-\frac{1}{2s}\frac{1}{N}\sum_{\langle ij\rangle}(\varphi^+_{i1}\varphi^+_{j2}-\varphi^+_{j1}\varphi^+_{i2})(e^{-ik_1r_j+ik_2r_i}-e^{-ik_1r_i+ik_2r_j})[t_1v^A_{k_1}u^B_{k_2}-t_2u^A_{k_1}v^B_{k_2}-t'v^A_{k_1}v^B_{k_2}+t'u^A_{k_1}u^B_{k_2}],$$

$$F_{k_1k_2}(\tau_2)=-\frac{1}{2s}\frac{1}{N}\sum_{\langle ij\rangle}(\varphi^+_{i1}\varphi^+_{j2}-\varphi^+_{j1}\varphi^+_{i2})(e^{-ik_1r_j+ik_2r_i}-e^{-ik_1r_i+ik_2r_j})[t_1v^A_{k_1}v^B_{k_2}+t_2u^A_{k_1}u^B_{k_2}+t'v^A_{k_1}u^B_{k_2}+t'u^A_{k_1}v^B_{k_2}], \tag{A20}$$

$$C_{k_1k_2}(\tau_2)=-\frac{1}{2s}\frac{1}{N}\sum_{\langle ij\rangle}(\varphi_{i1}\varphi_{j2}-\varphi_{j1}\varphi_{i2})(e^{-ik_1r_i+ik_2r_j}-e^{-ik_1r_j+ik_2r_i})[t_1u^B_{k_1}u^A_{k_2}+t_2v^B_{k_1}v^A_{k_2}-t'u^B_{k_1}v^A_{k_2}-t'v^B_{k_1}u^A_{k_2}],$$

$$D_{k_1k_2}(\tau_2)=-\frac{1}{2s}\frac{1}{N}\sum_{\langle ij\rangle}(\varphi_{i1}\varphi_{j2}-\varphi_{j1}\varphi_{i2})(e^{-ik_1r_i+ik_2r_j}-e^{-ik_1r_j+ik_2r_i})[t_1u^B_{k_1}v^A_{k_2}-t_2v^B_{k_1}u^A_{k_2}+t'u^B_{k_1}u^A_{k_2}-t'v^B_{k_1}v^A_{k_2}],$$

$$G_{k_1k_2}(\tau_2)=-\frac{1}{2s}\frac{1}{N}\sum_{\langle ij\rangle}(\varphi_{i1}\varphi_{j2}-\varphi_{j1}\varphi_{i2})(e^{-ik_1r_i+ik_2r_j}-e^{-ik_1r_j+ik_2r_i})[t_1v^B_{k_1}u^A_{k_2}-t_2u^B_{k_1}v^A_{k_2}-t'v^B_{k_1}v^A_{k_2}+t'u^B_{k_1}u^A_{k_2}],$$

$$I_{k_1k_2}(\tau_2)=-\frac{1}{2s}\frac{1}{N}\sum_{\langle ij\rangle}(\varphi_{i1}\varphi_{j2}-\varphi_{j1}\varphi_{i2})(e^{-ik_1r_i+ik_2r_j}-e^{-ik_1r_j+ik_2r_i})[t_1v^B_{k_1}v^A_{k_2}+t_2u^B_{k_1}u^A_{k_2}+t'v^B_{k_1}u^A_{k_2}+t'u^B_{k_1}v^A_{k_2}], \tag{A21}$$

where N is the number of lattice's sites. Integrating the fermions out we obtain the effective action S_{eff}

$$S_{\text{eff}} = -\ln\det W = -\operatorname{Tr}\ln W. \tag{A22}$$

Using the properties of the logarithm

$$\operatorname{Tr}\ln W = \operatorname{Tr}\ln(W^0 + W^{\text{int}}) = \operatorname{Tr}\ln W^0 + \operatorname{Tr}\ln[1 + (W^0)^{-1}W^{\text{int}}] \tag{A23}$$

we rewrite the effective action in the form

$$S_{\text{eff}} = -\operatorname{Tr}\ln[1 + (W^0)^{-1}W^{\text{int}}], \tag{A24}$$

where the term $\operatorname{Tr}\ln W^0$ does not depend on the Schwinger bosons and we have dropped it. Finally, we expand the effective action in powers of

$$X_{k_1k_2}(\tau_1,\tau_2) = \sum_q \int d\tau [W^0_{k_1q}(\tau_1,\tau)]^{-1} W^{\text{int}}_{qk_2}(\tau,\tau_2). \tag{A25}$$

The result is

$$S_{\text{eff}} = -\operatorname{Tr}X + \frac{1}{2}\operatorname{Tr}X^2 + \cdots. \tag{A26}$$

The inverse matrix $(W^0_{k_1k_2})^{-1}$ is given by

$$(W^0_{k_1k_2})^{-1}(\tau_1,\tau_2) = \begin{pmatrix} \delta_{k_1k_2}S^A_{1k_1}(\tau_1-\tau_2) & 0 & 0 & 0 \\ 0 & \delta_{k_1k_2}S^B_{1k_1}(\tau_1-\tau_2) & 0 & 0 \\ 0 & 0 & \delta_{k_1k_2}S^A_{2k_1}(\tau_1-\tau_2) & 0 \\ 0 & 0 & 0 & \delta_{k_1k_2}S^B_{2k_1}(\tau_1-\tau_2) \end{pmatrix}, \tag{A27}$$

where $S^\sigma_{lk}(\omega) = \frac{1}{-i\omega + E^\sigma_{lk}}$ ($\sigma = A$ or B, $l = 1$ or 2). Replacing Eq. (A18) into (A25), we end up with two terms for $X_{k_1k_2}$, one which is diagonal $X^{(1)}_{k_1k_2}$, and one with zero diagonal elements $X^{(2)}_{k_1k_2}$. Hence, one obtains for the trace of the matrix X

$$\operatorname{Tr}X = \operatorname{Tr}X^{(1)}, \tag{A28}$$

where

$$X^{(1)}_{k_1k_2}(\tau_1,\tau_2) = \begin{pmatrix} S^A_{1k_1}(\tau_1-\tau_2)K_{k_1k_2}(\tau_2) & 0 & 0 & 0 \\ 0 & S^B_{1k_1}(\tau_1-\tau_2)L_{k_1k_2}(\tau_2) & 0 & 0 \\ 0 & 0 & S^A_{2k_1}(\tau_1-\tau_2)N_{k_1k_2}(\tau_2) & 0 \\ 0 & 0 & 0 & S^B_{2k_1}(\tau_1-\tau_2)O_{k_1k_2}(\tau_2) \end{pmatrix} \tag{A29}$$

and the first term in the effective action (A26) is

$$S^{(1)}_{\text{eff}} = -\frac{1}{2s}\frac{1}{N}\sum_k \left(\sum_{\mu=1}^d \frac{\cos k_\mu}{d}\right)\int_0^\beta d\tau \sum_{\langle ij\rangle} (\varphi^+_{i\sigma}\varphi_{j\sigma} + \varphi^+_{j\sigma}\varphi_{i\sigma} - 4s)\{2t'[u^A_k v^A_k(n^A_{2k} - n^A_{1k}) + u^B_k v^B_k(n^B_{2k} - n^B_{1k})]$$
$$+ t_1[(u^A_k)^2 n^A_{1k} + (v^A_k)^2 n^A_{2k} + (u^B_k)^2 n^B_{1k} + (v^B_k)^2 n^B_{2k}] + t_2[(u^A_k)^2 n^A_{2k} + (v^A_k)^2 n^A_{1k} + (u^B_k)^2 n^B_{2k} + (v^B_k)^2 n^B_{1k}]\}. \tag{A30}$$

To calculate the contribution of $S^{(1)}_{\text{eff}}$ to the spin-stiffness constant ρ in Eq. (2.24) we use the Holstein-Primakoff representation for the Schwinger bosons

$$\varphi_{1i} = \varphi^+_{1i} = \sqrt{2s - \frac{s}{M}a^+_i a_i},$$

$$\varphi_{2i} = \sqrt{\frac{s}{M}}a_i, \quad \varphi^+_{2i} = \sqrt{\frac{s}{M}}a^+_i, \tag{A31}$$

and keep the terms quadratic with respect to the magnons a_i, a^+_i. The result is

$$\rho_1 = \frac{1}{2M}\frac{1}{N}\sum_k \left(\sum_{\mu=1}^d \frac{\cos k_\mu}{d}\right)(2t'\{[u^A_k v^A_k(n^A_{2k} - n^A_{1k}) + u^B_k v^B_k(n^B_{2k}$$
$$- n^B_{1k})]\} + t_1[(u^A_k)^2 n^A_{1k} + (v^A_k)^2 n^A_{2k} + (u^B_k)^2 n^B_{1k} + (v^B_k)^2 n^B_{2k}]$$
$$+ t_2[(u^A_k)^2 n^A_{2k} + (v^A_k)^2 n^A_{1k} + (u^B_k)^2 n^B_{2k} + (v^B_k)^2 n^B_{1k}]). \tag{A32}$$

Calculating the contribution of the second term in Eq. (A26) to the effective Hamiltonian (2.24) we account for the fact that X^1 matrix is quadratic with respect to magnons, hence it does not contribute. The contribution comes from $S^{(2)}_{s\text{-}f}$ (A5) which leads to the matrix $X^{(2)}$:

$$X^{(2)}_{k_1k_2}(\tau_1,\tau_2)=\begin{pmatrix} 0 & S^A_{1k_1}(\tau_1-\tau_2)A_{k_1k_2}(\tau_2) & 0 & S^A_{1k_1}(\tau_1-\tau_2)B_{k_1k_2}(\tau_2) \\ S^B_{1k_1}(\tau_1-\tau_2)C_{k_1k_2}(\tau_2) & 0 & S^B_{1k_1}(\tau_1-\tau_2)D_{k_1k_2}(\tau_2) & 0 \\ 0 & S^A_{2k_1}(\tau_1-\tau_2)E_{k_1k_2}(\tau_2) & 0 & S^A_{2k_1}(\tau_1-\tau_2)F_{k_1k_2}(\tau_2) \\ S^B_{2k_1}(\tau_1-\tau_2)G_{k_1k_2}(\tau_2) & 0 & S^B_{2k_1}(\tau_1-\tau_2)I_{k_1k_2}(\tau_2) & 0 \end{pmatrix}. \quad \text{(A33)}$$

After some algebra we arrive at the following representation of the second term in Eq. (A26)

$$S^{(2)}_{\text{eff}}=\int d\tau_1 d\tau_2 \sum_{k_1k_2}[S^A_{1k_1}(\tau_1-\tau_2)A_{k_1k_2}(\tau_2)S^B_{1k_2}(\tau_2-\tau_1)C_{k_2k_1}(\tau_1)+S^A_{1k_1}(\tau_1-\tau_2)B_{k_1k_2}(\tau_2)S^B_{2k_2}(\tau_2-\tau_1)G_{k_2k_1}(\tau_1)+S^A_{2k_1}(\tau_1-\tau_2)E_{k_1k_2}(\tau_2)S^B_{1k_2}(\tau_2-\tau_1)D_{k_2k_1}(\tau_1)+S^A_{2k_1}(\tau_1-\tau_2)F_{k_1k_2}(\tau_2)S^B_{2k_2}(\tau_2-\tau_1)I_{k_2k_1}(\tau_1)]. \quad \text{(A34)}$$

Switching from imaginary time τ representation to frequency ω representation we calculate the expressions in the small ω approximation. The result is a

$$S^A_{lk_1}(\tau_1-\tau_2)S^B_{l'k_2}(\tau_1-\tau_2)\simeq\delta(\tau_1-\tau_2)\int\frac{d\omega}{2\pi}S^A_{lk_1}(\omega)S^B_{l'k_2}(\omega). \quad \text{(A35)}$$

Next we make a change of wave vectors variables $k_1=q+\frac{1}{2}k$, $k_1=q-\frac{1}{2}k$, and calculate the expressions in small wave-vector k approximation. The expression (A34) calculated in small frequency and small wave-vector approximation has the form

$$S^{(2)}_{\text{eff}}=\int\frac{d\omega}{2\pi s^2}\frac{1}{N}\sum_q\left(\sum_{\mu=1}^{3}\frac{\sin^2 q_\mu}{3}\right)\sum_{ij}[(\varphi^+_{i1}\varphi^+_{j2}-\varphi^+_{j1}\varphi^+_{i2})(\varphi_{i1}\varphi_{j2}-\varphi_{j1}\varphi_{i2})][S^A_{1q}(\omega)S^B_{1q}(\omega)(t_1u^A_qu^B_q+t_2v^A_qv^B_q-t'u^A_qv^B_q-t'v^A_qu^B_q)^2+S^A_{1q}(\omega)S^B_{2q}(\omega)(t_1u^A_qv^B_q-t_2v^A_qu^B_q+t'u^A_qu^B_q-t'v^A_qv^B_q)^2+S^A_{2q}(\omega)S^B_{1q}(\omega)(t_1v^A_qu^B_q-t_2u^A_qv^B_q-t'v^A_qv^B_q+t'u^A_qu^B_q)^2+S^A_{2q}(\omega)S^B_{2q}(\omega)\times(t_1v^A_qv^B_q+t_2u^A_qu^B_q+t'v^A_qu^B_q+t'u^A_qv^B_q)^2]. \quad \text{(A36)}$$

Our third step is to express the products of the Green functions, in the above equation, in terms of the Fermi function $n(E)=1/(e^E+1)$

$$\int\frac{d\omega}{2\pi}S^A_{1q}(\omega)S^B_{1q}(\omega)=\frac{n(E^B_{1q})-n(E^A_{1q})}{E^B_{1q}-E^A_{1q}}, \quad \text{(A37)}$$

$$\int\frac{d\omega}{2\pi}S^A_{1q}(\omega)S^B_{2q}(\omega)=\frac{n(E^B_{2q})-n(E^A_{1q})}{E^B_{2q}-E^A_{1q}}, \quad \text{(A38)}$$

$$\int\frac{d\omega}{2\pi}S^A_{2q}(\omega)S^B_{1q}(\omega)=\frac{n(E^B_{1q})-n(E^A_{2q})}{E^B_{1q}-E^A_{2q}}, \quad \text{(A39)}$$

$$\int\frac{d\omega}{2\pi}S^A_{2q}(\omega)S^B_{2q}(\omega)=\frac{n(E^B_{2q})-n(E^A_{2q})}{E^B_{2q}-E^A_{2q}}. \quad \text{(A40)}$$

Finally we use the representation of the Schwinger bosons (A31). To calculate the contribution to the spin-stiffness constant it is enough to keep only the quadratic terms with respect to magnons

$$\rho_2=\frac{2}{M}\frac{1}{V}\sum_q\left(\sum_{\mu=1}^{d}\frac{\sin^2 q_\mu}{d}\right)\left[(t_1u^A_qu^B_q+t_2v^A_qv^B_q-t'u^A_qv^B_q-t'v^A_qu^B_q)^2\left(\frac{n(E^B_{1q})-n(E^A_{1q})}{E^B_{1q}-E^A_{1q}}\right)+(t_1u^A_qv^B_q-t_2v^A_qu^B_q+t'u^A_qu^B_q-t'v^A_qv^B_q)^2\left(\frac{n(E^B_{2q})-n(E^A_{1q})}{E^B_{2q}-E^A_{1q}}\right)+(t_1v^A_qu^B_q-t_2u^A_qv^B_q-t'v^A_qv^B_q+t'u^A_qu^B_q)^2\left(\frac{n(E^B_{1q})-n(E^A_{2q})}{E^B_{1q}-E^A_{2q}}\right)+(t_1v^A_qv^B_q+t_2u^A_qu^B_q+t'v^A_qu^B_q+t'u^A_qv^B_q)^2\left(\frac{n(E^B_{2q})-n(E^A_{2q})}{E^B_{2q}-E^A_{2q}}\right)\right]. \quad \text{(A41)}$$

The spin-stiffness constant in the effective action (2.24) is a sum of the expressions (A32) and (A41)

$$\rho = \left\{ \frac{t_1}{2M}\frac{1}{V}\sum_k \left(\sum_{\mu=1}^{d} \frac{\cos k_\mu}{d} \right) [(u_k^A)^2 n_{1k}^A + (v_k^A)^2 n_{2k}^A + (u_k^B)^2 n_{1k}^B + (v_k^B)^2 n_{2k}^B] + \frac{t_2}{2M}\frac{1}{V}\sum_k \left(\sum_{\mu=1}^{d} \frac{\cos k_\mu}{d} \right) [(u_k^A)^2 n_{2k}^A + (v_k^A)^2 n_{1k}^A + (u_k^B)^2 n_{2k}^B \right.$$
$$+ (v_k^B)^2 n_{1k}^B] + \frac{t'}{M}\frac{1}{V}\sum_k \left(\sum_{\mu=1}^{d} \frac{\cos k_\mu}{d} \right) [u_k^A v_k^A (n_{2k}^A - n_{1k}^A) + u_k^B v_k^B (n_{2k}^B - n_{1k}^B)] + \frac{2}{M}\frac{1}{V}\sum_k \left(\sum_{\mu=1}^{d} \frac{\sin^2 k_\mu}{d} \right) \Bigg[(t_1 u_k^A u_k^B + t_2 v_k^A v_k^B - t' u_k^A v_k^B$$
$$- t' v_k^A u_k^B)^2 \left(\frac{n_{1k}^B - n_{1k}^A}{E_{1k}^B - E_{1k}^A} \right) + (t_1 u_k^A v_k^B - t_2 v_k^A u_k^B + t' u_k^A u_k^B - t' v_k^A v_k^B)^2 \left(\frac{n_{2k}^B - n_{1k}^A}{E_{2k}^B - E_{1k}^A} \right) + (t_1 v_k^A u_k^B - t_2 u_k^A v_k^B - t' v_k^A v_k^B$$
$$\left. + t' u_k^A u_k^B)^2 \left(\frac{n_{1k}^B - n_{2k}^A}{E_{1k}^B - E_{2k}^A} \right) + (t_1 v_k^A v_k^B + t_2 u_k^A u_k^B + t' v_k^A u_k^B + t' u_k^A v_k^B)^2 \left(\frac{n_{2k}^B - n_{2k}^A}{E_{2k}^B - E_{2k}^A} \right) \Bigg] \right\}. \quad \text{(A42)}$$

*naoum@phys.uni-sofia.bg

[1] E. Dagotto, *Nanoscale Phase Separation and Colossal Magnetoresistance* (Springer-Verlag, Berlin, 2003), and references therein.

[2] C. Zener, Phys. Rev. **81**, 440 (1951).

[3] H. Ohno *et al.*, Appl. Phys. Lett. **69**, 363 (1996).

[4] S. Yunoki, J. Hu, A. L. Malvezzi, A. Moreo, N. Furukawa, and E. Dagotto, Phys. Rev. Lett. **80**, 845 (1998).

[5] J. L. Alonso, J. A. Capitan, L. A. Fernandez, F. Guinea, and V. Martin-Mayor, Phys. Rev. B **64**, 054408 (2001).

[6] A. Chattopadhyay, A. J. Millis, and S. Das Sarma, Phys. Rev. B **64**, 012416 (2001).

[7] Daniel P. Arovas and Francisco Guinea, Phys. Rev. B **58**, 9150 (1998).

[8] D. Pekker, S. Mukhopadhyay, N. Trivedi, and P. M. Goldbart, Phys. Rev. B **72**, 075118 (2005).

[9] M. Kagan, D. Khomskii, and M. Mostovoy, Eur. Phys. J. B **12**, 217 (1999).

[10] Shun-Qing Shen and Z. D. Wang, Phys. Rev. B **61**, 9532 (2000).

[11] Takashi Hotta, Mohammad Moraghebi, Adrian Feiguin, Adriana Moreo, Seiji Yunoki, and Elbio Dagotto, Phys. Rev. Lett. **90**, 247203 (2003).

[12] H. Roder, R. R. P. Singh, and J. Zang, Phys. Rev. B **56**, 5084 (1997).

[13] N. Furukawa, J. Phys. Soc. Jpn. **64**, 2754 (1995).

[14] A. J. Millis, P. B. Littlewood, and B. I. Shraiman, Phys. Rev. Lett. **74**, 5144 (1995).

[15] F. Popescu, C. Şen, and E. Dagotto, Phys. Rev. B **73**, 180404(R) (2006).

[16] M. Stier and W. Nolting, Phys. Rev. B **75**, 144409 (2007).

[17] N. D. Mermin and H. Wagner, Phys. Rev. Lett. **17**, 1133 (1966).

[18] J. R. Schrieffer and P. A. Wolf, Phys. Rev. **149**, 491 (1966).

[19] E. L. Nagaev, Phys. Rev. B **58**, 827 (1998).

[20] D. P. Arovas and A. Auerbach, Phys. Rev. B **38**, 316 (1988).

[21] D. Yoshioka, J. Phys. Soc. Jpn. **58**, 32 (1989).

[22] F. Popescu, Y. Yildirim, G. Alvarez, A. Moreo, and E. Dagotto, Phys. Rev. B **73**, 075206 (2006).